

Mode-coupling Cerenkov sum-frequency-generation in a multimode planar waveguide

Changdong Chen,¹ Jie Su,¹ Yong Zhang,^{1,2} Ping Xu,^{1,a)} Xiaopeng Hu,^{1,a)} Gang Zhao,¹ Yanhua Liu,¹ Xinjie Lv,¹ and Shining Zhu¹

¹Department of Physics, National Laboratory of Solid State Microstructures, Nanjing University, Nanjing 210093, People's Republic of China

²School of Modern Engineering and Applied Science, Nanjing University, Nanjing, 210093, People's Republic of China

(Received 28 July 2010; accepted 4 October 2010; published online 22 October 2010)

We present experimental and theoretical studies of the mode-coupling Cerenkov sum-frequency radiations in a multimode LiNbO₃ planar waveguide. The radiations result from the coupling of different guided modes of the fundamental wave, which have the same optical frequencies but different propagation constants. At the same time, scattering-involved Cerenkov sum-frequency-generation was also observed and discussed. Our theoretical predictions are in well accordance with the experimental results. © 2010 American Institute of Physics.

[doi:10.1063/1.3505359]

The conventional Cerenkov radiation is due to a charged particle moving faster than the velocity of the light in medium.¹ The coherent radiation is emitted at the Cerenkov angle defined by $\theta_c = \arccos(v'/v)$, where v' is the phase velocity of the radiation wave and v the speed of the particle. In optical waveguides, such an emission can also occur via a second-order nonlinear process.^{2–14} In 1970, Tien *et al.* reported Cerenkov second harmonic generation (SHG) in ZnS film.² Since then, the applications^{3,4} and theoretical investigations of Cerenkov SHG (Refs. 5–7) have been described in detail. Furthermore, Cerenkov sum-frequency generation (SFG) (Refs. 8–10) and different-frequency¹¹ also attracted increasing attentions. More recently, backward Cerenkov emission,¹² quasiphase-matched Cerenkov radiation¹³ and Cerenkov type SHG in the bulk crystals^{15,16} have also been reported.

As well known, several modes with different propagation constants can be supported in a multimode waveguide. For nonlinear processes in a multimode waveguide, the material dispersion could cause a wave-vector mismatch between the fundamental and the harmonic. This mismatch could be compensated by either the mode dispersion¹⁷ or Cerenkov phase-matching^{2–14} and the latter is more efficient. Related works only mentioned the Cerenkov radiations from the coupling between the same spatial modes and there have been no reports on the Cerenkov radiations resulted from the coupling between different spatial modes till now.

In this letter, we present a type of Cerenkov radiation generated from a multimode planar waveguide. Besides the Cerenkov SHG from the identical spatial modes, the Cerenkov SFG induced by the coupling of different guided modes was observed. In addition, the elastic scattering wave of the fundamental was also observed to participate in the radiations.

The sample we used was a Z-cut LiNbO₃ (LN) planar waveguide fabricated using a proton-exchange method. The LN wafer with 0.5 mm thickness was first immersed into the

benzoic acid and proton-exchanged at 220 °C for 2 h. Subsequently, the sample was subjected to annealing treatment at 380 °C for 5 h, which could recover the nonlinear coefficient and create a graded-index layer in the waveguide.¹⁸ In addition, based on the fabrication conditions, there are three TM modes at 1064 nm in the waveguide calculated using the finite element method.¹⁹ The effective refractive indexes $N_{eff_i}(i=0,1,2)$ are 2.1950, 2.1743, and 2.1604, corresponding to TM₀, TM₁, and TM₂ modes, respectively.

We performed experimental study of Cerenkov radiation as shown in Fig. 1. The fundamental is a 90 ns pulsed Q-switched Nd:YAG laser operating at 1064 nm and the pulse repetition is adjustable within the range 1–50 kHz. A proton-exchanged Z-cut LN waveguide only maintains TM modes,²⁰ so the z -polarized fundamental beam was focused into the y face of the waveguide by a cylindrical lens with a focal length of 3 mm. The generated second harmonic (SH) radiation was projected onto a screen placed 128 mm away from the end face of the sample. Filter M₁ was used to filter out the residual IR beam. The operating temperature was kept at 25 °C.

When the fundamental was coupled into the waveguide, a pattern composed of green spots and arcs appeared on the screen, as shown in Fig. 2(a). All the spots labeled with ①–⑥ may result from the Cerenkov up-conversion. As shown in Fig. 3, the phase-matching condition can be written as

$$|\vec{\beta}_i(\omega) + \vec{\beta}_j(\omega)| = |\vec{k}_{i,j}(2\omega)| \cos \theta_{i,j}, \quad (1)$$

where $\vec{\beta}_{i(j)}(\omega) = N_{eff_{i(j)}}(\omega) \vec{k}_0(\omega)$ is the propagation constant of TM_{*i(j)*} mode at 1064 nm, $\vec{k}_{i,j}(2\omega) = n_{i,j}(2\omega) \vec{k}_0(2\omega)$ is the

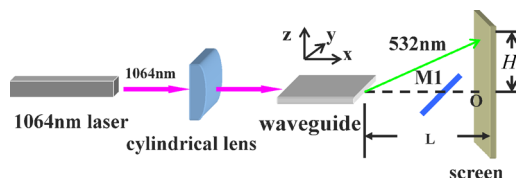


FIG. 1. (Color online) Simplified layout of the experimental setup.

^{a)}Authors to whom correspondence should be addressed. Electronic addresses: pingxu520@nju.edu.cn and xphu@nju.edu.cn.

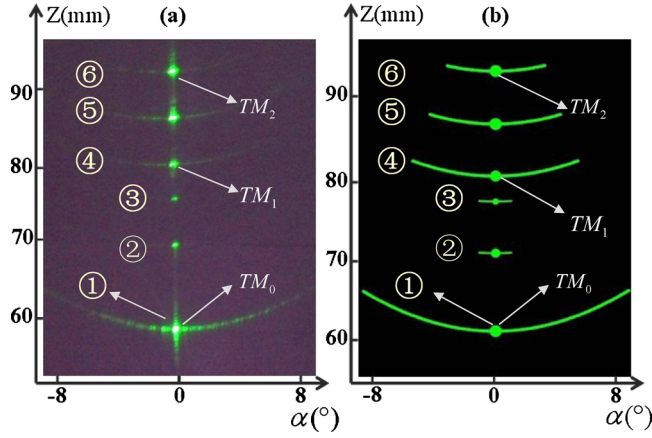


FIG. 2. (Color online) Projection of Cerenkov SHG and Cerenkov SFG patterns on the screen measured (a) and the calculated distribution (b). Spots ①, ④, ⑥ were induced by Cerenkov SHG and the other three spots ②, ③, and ⑤ resulted from Cerenkov SFG.

wave vector of Cerenkov SH wave in the substrate, $n_{i,j}(2\omega)$ is the refractive index of SH in the substrate and $\theta_{i,j}$ is the Cerenkov angle.

If $i=j$, i.e., two identical spatial modes get involved, that is conventional Cerenkov SHG. Thus Eq. (1) can be written as

$$|2\vec{\beta}_i(\omega)| = |\vec{k}_i(2\omega)| \cos \theta_i. \quad (2)$$

On the basis of our calculations, we found that the SH spots ①, ④, and ⑥ resulted from TM_0 , TM_1 , and TM_2 modes, respectively. We defined H_i as the vertical distance from the position of the Cerenkov spot labeled as i to the x-y plane on the screen. As shown in the left part labeled ‘‘Cerenkov SHG’’ of Table I, the measured H_1 , H_4 and H_6 were well consistent with the theoretical calculations.

If $i \neq j$, can different guided modes couple efficiently to generate Cerenkov radiations? As shown in Fig. 2(a), besides the SH spots ①, ④, and ⑥ on the screen, there are other three spots which located among them. Also, we use Eq. (1) and define $SFG[i,j]$ as the Cerenkov SFG between TM_i and TM_j modes. By numerical calculations, we found that the spatial distributions of the three guide modes TM_0 , TM_1 , and TM_2 can overlap with each other to generate Cerenkov SFG radiations. The corresponding Cerenkov SFG wave with larger $|\vec{\beta}_i(\omega) + \vec{\beta}_j(\omega)|$ is emitted along a bigger angle. As shown in Fig. 2(a), the spots ②, ③, and ⑤, from the bottom up, resulted from $SFG[0,1]$, $SFG[0,2]$, and $SFG[1,2]$, respectively. Theoretical predictions were in well accordance with the experimental results and the average error was about 2.79%, as the data shown in the right part labeled ‘‘Cerenkov SFG’’ of

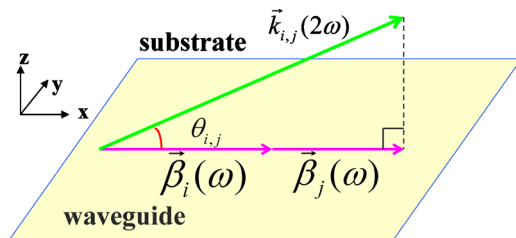


FIG. 3. (Color online) Geometry of the phase-matching process in Cerenkov SHG ($i=j$) and Cerenkov SFG ($i \neq j$) with the i th-order and j th-order guide modes.

TABLE I. The experimental (H_E) and theoretical data (H_T) of H_i for both Cerenkov SHG (left part) and SFG (right part) processes.

H_i	Cerenkov SHG		Cerenkov SFG		
	H_E (mm)	H_T (mm)	H_i	H_E (mm)	H_T (mm)
H_1	58.0	61.4	H_2	68.9	71.1
H_4	80.4	80.8	H_3	74.4	77.6
H_6	94.4	93.9	H_5	86.3	87.3

Table I. These three spots were induced by the coupling between two different guide modes, which have the same frequencies but different propagation constants, and we call that mode-coupling Cerenkov SFG. In a more general case, for a multimode waveguide with n guided modes, there are totally $n(n+1)/2$ Cerenkov radiation spots, n for Cerenkov SHG and $n(n-1)/2$ for SFG, respectively.

The Cerenkov SH spots intensity follows $I_{SHG} \propto I_i^2(\omega)$, in which $I_i(\omega)$ is the fundamental power coupled into TM_i mode ($i=0,1,2$). In our experiment, we measured the intensity of the SH spots and deduced that $I_0:I_1:I_2=1.5:1:1.3$. The intensity of Cerenkov SFG follows $I_{SFG} \propto \gamma_{jk}^2 I_j(\omega) I_k(\omega)$, in which γ_{jk} is the overlapping of TM_j and TM_k modes. Numerical calculations show that $\gamma_{12}:\gamma_{02}:\gamma_{01}=9:3:5$, taking the fundamental power of the guided mode into account, we can obtain that the relative intensity of the SFG spots was in compliance with 6:1:2.1, which follows ⑤>②>③ as shown in Fig. 2(a). Actually, the calculated intensity of these SFG spots differs slightly with experimental result which was about 5.8:1:2, because one guided mode will involve in multiple nonlinear processes that compete with each other, and this is not included in the discussions above.

Scattering happens when lights travel through matters. In the waveguide, defects and other imperfections inside the waveguide can cause elastic scattering of the guided waves. The scattering involved Cerenkov radiation may occur as well. In Fig. 2(a), one can find that there are arcs tangent with all the Cerenkov radiation spots. The arcs around spots ①, ④, and ⑥ are induced by the interaction of the guide modes and their own elastic scattering wave.¹³ Furthermore, scattering can also participate in the Cerenkov SFG, which results in the arcs around spots ②, ③, and ⑤, named scattering-involved mode-coupling Cerenkov SFG. The corresponding phase-matching geometry is shown in Fig. 4 and can be written as

$$\begin{aligned} & \sqrt{|\vec{\beta}_i(\omega)|^2 + |\vec{\beta}'_j(\omega)|^2 + 2 \cdot |\vec{\beta}_i(\omega)| \cdot |\vec{\beta}'_j(\omega)| \cdot \cos \alpha} \\ & = |\vec{k}'(2\omega)| \cos \theta'_{i,j}, \end{aligned} \quad (3)$$

where $\vec{\beta}'_j(\omega)$ is the propagation constant of the scattering light of TM_j mode at 1064 nm, $\vec{k}'(2\omega)$ is wave vector of the SFG in substrate, $\theta'_{i,j}$ is the Cerenkov angle and α is the angle between the scattering light $\vec{\beta}'_j$ and the fundamental $\vec{\beta}_i$. The simulated results were shown in Fig. 2(b). The arcs symmetrically distributed around the Cerenkov spots due to the symmetrical distributions of the scattered fundamental waves in the waveguide. Theoretically, the Cerenkov arcs should be continuous because of the continuous distribution of the scattering light. We speculate that the discrete dots observed in the arcs are due to the defects on the output facet, as shown

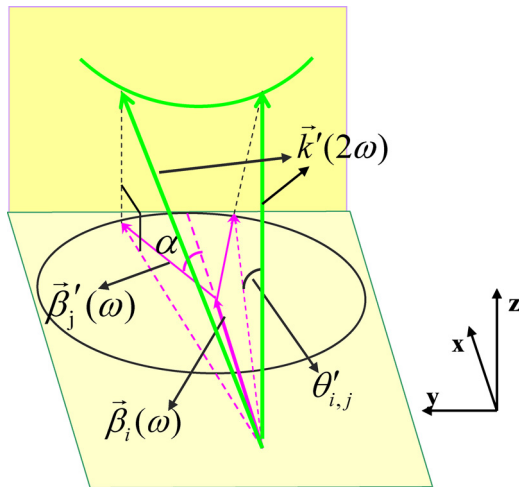


FIG. 4. (Color online) The phase-matching geometry for scattering-involved Cerenkov SHG arcs ($i=j$) and Cerenkov SFG arcs ($i \neq j$) with the i th-order guide mode and the scattering light of j th-mode.

in Fig. 2(a). In Fig. 2(b), our numerical simulations shown that the scattered light distributed from $\alpha=-8^\circ$ to $\alpha=8^\circ$ for the SH spot ①, while the scattering for the other spots was limited in a very small range. The intensity of each arc is proportional to the intensity of the corresponding Cerenkov spot as well as the scattering strength.

In summary, we have reported both the Cerenkov SHG from two identical guide modes and the mode-coupling Cerenkov SFG from two different guided modes in a multimode LN planar waveguide. In addition, elastic scattering of the fundamental can also participate in the mode-coupling Cerenkov radiation. Theoretical analyses as well as numerical calculations were also performed to verify the experimental results.

This work was supported by the National Natural Science Foundations of China under Contract Nos. 10904066, 11004097, and 10776011 and the State Key Program for Basic Research of China (Grant Nos. 2006CB921804 and 2010CB630703).

- ¹P. A. Cherenkov, Dokl. Akad. Nauk SSSR **2**, 451 (1934).
- ²P. K. Tien, R. Ulrich, and R. J. Martin, *Appl. Phys. Lett.* **17**, 447 (1970).
- ³N. A. Sanford and W. C. Robinson, *Opt. Lett.* **12**, 445 (1987).
- ⁴R. Ramponi, M. Marangoni, R. Osellame, and V. Russo, *Opt. Commun.* **159**, 37 (1999).
- ⁵H. Tamada, *IEEE J. Quantum Electron.* **27**, 502 (1991).
- ⁶T. Suhara, T. Morimoto, and H. Nishihara, *IEEE J. Quantum Electron.* **29**, 525 (1993).
- ⁷K. Hayata, K. Yanagawa, and M. Koshiba, *Appl. Phys. Lett.* **56**, 206 (1990).
- ⁸N. A. Sanford and J. M. Connors, *J. Appl. Phys.* **65**, 1429 (1989).
- ⁹K. Hayata and M. Koshiba, *J. Opt. Soc. Am. B* **8**, 449 (1991).
- ¹⁰K. Yamamoto, H. Yamamoto, and T. Taniuchi, *Appl. Phys. Lett.* **58**, 1227 (1991).
- ¹¹K. Suizu, K. Koketsu, T. Shibuya, T. Tsutsui, T. Akiba, and K. Kawase, *Opt. Express* **17**, 6676 (2009).
- ¹²C. Luo, M. Ibanescu, S. G. Johnson, and J. D. Joannopoulos, *Science* **299**, 368 (2003).
- ¹³Y. Zhang, Z. D. Gao, Z. Qi, S. N. Zhu, and N. B. Ming, *Phys. Rev. Lett.* **100**, 163904 (2008).
- ¹⁴M. J. Li, M. De Micheli, Q. He, and D. B. Ostrowsky, *IEEE J. Quantum Electron.* **26**, 1384 (1990).
- ¹⁵A. Fragemann, V. Pasiskevicius, and F. Laurell, *Appl. Phys. Lett.* **85**, 375 (2004).
- ¹⁶Y. Sheng, S. M. Saltiel, W. Krolikowski, A. Arie, K. Koynov, and Y. S. Kivshar, *Opt. Lett.* **35**, 1317 (2010).
- ¹⁷K. Moutzouris, S. Venugopal Rao, and M. Ebrahimzadeh, *Appl. Phys. Lett.* **83**, 620 (2003).
- ¹⁸P. G. Suchoski, T. K. Findakly, and F. J. Leonberger, *Opt. Lett.* **13**, 1050 (1988).
- ¹⁹B. M. A. Rahman and J. B. Davies, *J. Lightwave Technol.* **2**, 682 (1984).
- ²⁰J. L. Jackel, C. E. Rice, and J. J. Veselka, *Appl. Phys. Lett.* **41**, 607 (1982).